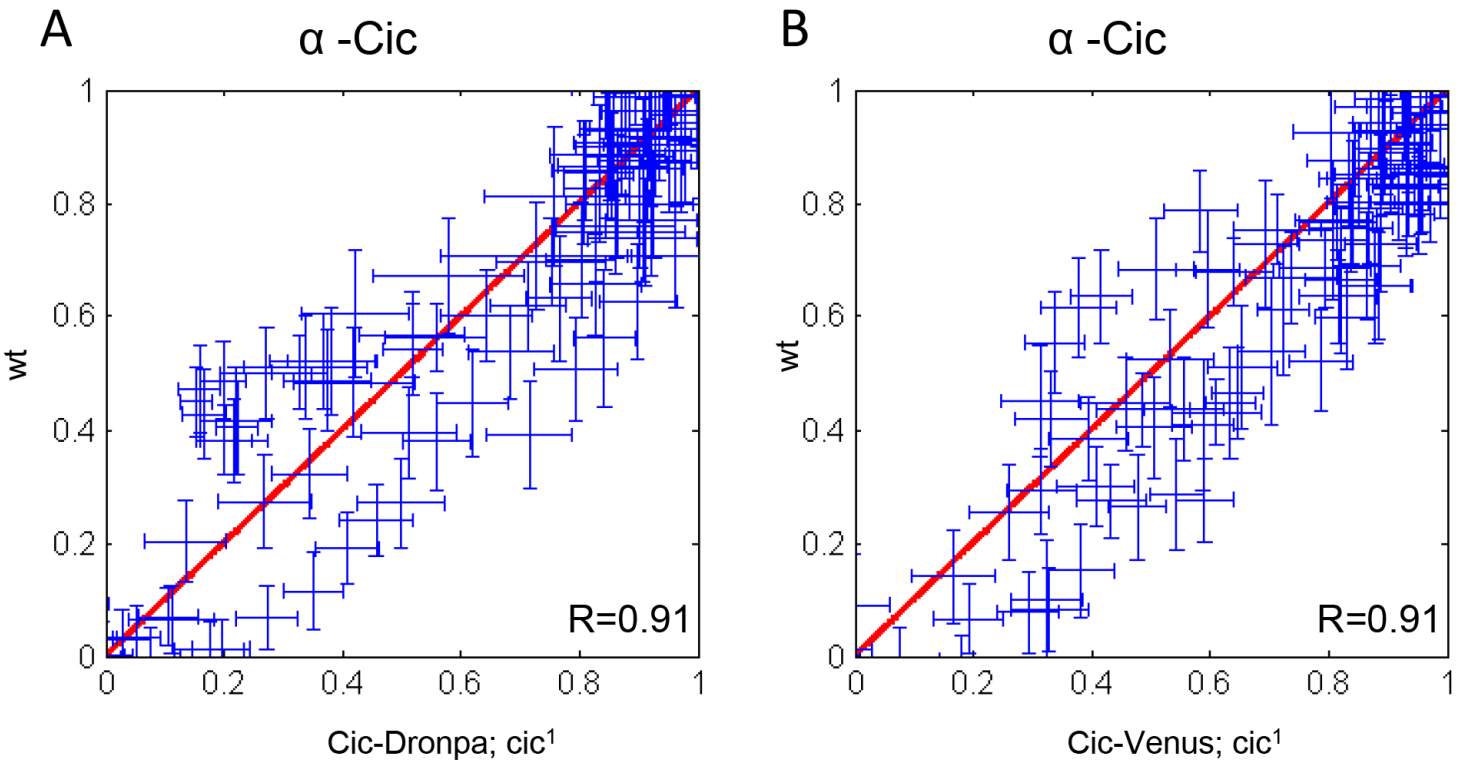

Fig. S1. Comparison of the spatial distributions of Cic-Dronpa and Cic-Venus fusion proteins with the spatial distribution of endogenous Cic. Fly lines were created containing copies of the tagged molecule allele in a background homozygous for the hypomorphic allele *cic*^{1}. Embryos from these lines and control embryos were fixed and stained with an anti-Cic antibody. The Cic gradients along the AP axis during early nuclear cycle 14 were quantified as described previously (Kim et al., 2011b) and compared using a correlation coefficient. (**A**) Spatial distributions of Cic-Dronpa and endogenous Cic are linearly correlated (R=0.91, based on the analysis of normalized gradients in fixed embryos; n_{wt}=17, $n_{Cic\text{-}Dronpa}$=12). (**B**) Spatial distributions of Cic-Venus and endogenous Cic are linearly correlated (R=0.91, based on the analysis of normalized gradients in fixed embryos; n_{wt}=9, $n_{Cic\text{-}Venus}$=24).

Appendix S1

Analysis of FRAP kinetics

When interphase nuclei are bleached, nuclear levels of Cic first increase rapidly, but then recover only a fraction of their pre-bleached value before the next mitosis, which limits the time window for collecting the FRAP kinetics data (Fig. 3B,C). Incomplete recovery of nuclear Cic on this time scale is in contrast to complete recovery observed in FRAP kinetics of other transcription factors in the same experimental system (Gregor et al., 2007; DeLotto et al., 2007), and raises the possibility that Cic levels in the cytoplasm are limiting. This seems unlikely, however, as we observe constant cytoplasmic levels throughout the FRAP. Furthermore, previously bleached nuclei recover to levels indistinguishable from their unbleached neighbors after mitosis (Fig. 3B). This suggests the existence of two populations of Cic molecules in the nucleus: a mobile pool that exchanges relatively rapidly with the cytoplasm during interphase; and a pool that exchanges with the cytoplasm either on a longer time scale or only during mitosis. This slowly exchanging population might reflect DNA-bound protein.

To analyze the FRAP data, we use a mathematical model with three distinct molecular pools: the nuclear mobile pool, the nuclear immobile pool and the cytoplasmic pool. Nucleocytoplasmic shuttling of the nuclear mobile pool was modeled by first-order kinetics. The cytoplasmic levels remain constant during the duration of the experiment. Thus, the cytoplasmic compartment was modeled as a constant concentration pool. We assumed that there is no exchange between the mobile and immobile nuclear pools during the duration of the experiment. These assumptions lead to the following equations for the dynamics during the time course of the FRAP experiment:

$$\frac{dN_{mob}(t)}{dt} = k_{in}C - k_{out}N_{mob}(t),$$

$$\frac{dN_{im}(t)}{dt} = 0$$

and

$$\frac{dC(t)}{dt} = 0,$$

where N_{mob}, N_{im} and C denote the nuclear mobile pool, nuclear immobile pool and cytoplasmic pool concentrations, respectively. We assumed that prior to bleaching, the mobile part of the nuclear pool is in quasi equilibrium with the cytoplasmic pool, and that both mobile and immobile nuclear pools are bleached to the same extent, denoted by α. This leads to the following initial conditions for the model:

$$N_{mob}(0) = \alpha N_{mob}^{ss} = \alpha \frac{C k_{in}}{k_{out}}$$

$$N_{im}(0) = \alpha N_{im}$$

$$C(0) = C.$$

Solving the model, we obtained the following recovery profile:

$$N(t) = N_{mob}(t) + N_{im}(t) = \alpha N_{im} + \frac{C k_{in}}{k_{out}}(1 - (1 - \alpha)\exp(-k_{out}t)).$$

A function of the form $N(t) = Q + Pexp(-bt)$ was used to fit the FRAP data using a nonlinear least squares method, and k_{out} and k_{in} can be extracted from the fit coefficients 'b' and 'P', respectively. Mean values of k_{in} and k_{out} for the two different genetic backgrounds were compared using a paired *t*-test.

Computational model

The computational model for the spatiotemporal dynamics of Cic was based on previously published models for the Dorsal and Bicoid gradients (Kanodia et al., 2009; Kavousanakis et al., 2010). During interphase, the embryo was modeled as a periodic arrangement of units comprising a nucleus and an associated cytoplasmic island, the state of each unit was described by two variables – the nuclear and cytoplasmic concentrations of Capicua. Our observations suggested that lateral transport between compartments could be neglected (data not shown). As a consequence, the only source of spatial variations in the model comes from the spatial variations of nuclear import and export rates, which were estimated from the combination of the spatial pattern of dpERK along the AP axis and the experimentally measured import and export

rates in the mid-body of the embryo at two distinct levels of RTK signaling (in the wild type and *torso* gain-of-function mutant).

The model for each unit accounts for nuclear import and export, as well as for cytoplasmic synthesis and degradation. We assumed that fluxes in and out of the nucleus are proportional to its surface area, estimated from previously published results. Dynamic equations for a single unit 'j' during interphase of nuclear cycle 'i' are given by:

$$\frac{d}{dt}\left(V_{c,i}C_i^j(t)\right) = \bar{k}_{out}^j A_{n,i} N_i^j(t) - \bar{k}_{in}^j A_{n,i} C_i^j(t) + qV_{c,i} - V_{c,i}\bar{k}_{deg} C_i^j(t)$$

and

$$\frac{d}{dt}\left(V_{n,i}N_i^j(t)\right) = -\bar{k}_{out}^j A_{n,i} N_i^j(t) + \bar{k}_{in}^j A_{n,i} C_i^j(t),$$

where $C_i^j(t)$ and $N_i^j(t)$ denote the cytoplasmic and nuclear concentrations in unit 'j' during the 'i-th' interphase. $V_{n,i}$ and $V_{c,i}$ are the volumes of the nuclear and cytoplasmic compartments, respectively. $A_{n,i}$ is the nuclear surface area at nuclear cycle 'i'. $\bar{k}_{in}^j$ *and* $\bar{k}_{out}^j$ denote the surface reaction rate constants for the nuclear import and export, respectively. q and $\bar{k}_{deg}$ are the rate of protein synthesis in the cytoplasm and the rate constant of cytoplasmic degradation. For simplicity, we assumed that the volumes of nuclear and cytoplasmic compartments remain constant during a particular interphase.

Choosing steady-state cytoplasmic concentration as the unit of concentration, we removed the rate of protein synthesis from the list of parameters. The remaining parameters were $\bar{k}_{in}^j, \bar{k}_{out}^j$ and $\bar{k}_{deg}$, which were estimated from our experimental results as follows. For the mid-body region of the embryo, $\bar{k}_{in}^j, \bar{k}_{out}^j$ can be related to the measured nuclear import and export rates, k_{in} and k_{out}:

$$\bar{k}_{in}^j = \frac{k_{in}V_{n\_13}}{A_{n\ 13}}, \qquad \bar{k}_{out}^j = \frac{k_{out}V_{n\_13}}{A_{n\ 13}}$$

Our FRAP measurements provided $\bar{k}_{in}^{j}$ and $\bar{k}_{out}^{j}$ in the midbody of the wild-type and Torso gain-of-function embryos. A linear approximation based on these values yields $\bar{k}_{in}^{j}$ and $\bar{k}_{out}^{j}$ for all other values of dpERK signal. In this way, we obtained a profile for $\bar{k}_{in}^{j}$ and $\bar{k}_{out}^{j}$ along the AP axis of the embryo. We assumed these spatial profiles of import and export to remain constant throughout nuclear cycles.

The remaining parameter, $\bar{k}_{deg}$, was obtained from our measurements of the Cic lifetime in the midbody of wild-type embryos. The degradation rate obtained from the lifetime assay, k_{deg}, corresponds to an effective degradation rate, which does not distinguish between nuclear and cytoplasmic compartments. We used a single unit from our model to optimize a value of cytoplasmic $\bar{k}_{deg}$ that would give rise to the measured effective degradation rate k_{deg}. The corresponding $\bar{k}_{deg}$ is found to be $1.4k_{deg}$.

Once all the parameters were obtained for each unit along the AP axis, the equations were solved numerically, using the variable time step Runge-Kutta method ode45 solver in MATLAB. Finally, during mitosis, the nuclear volume compartments are assumed to disappear and their contents are released into the cytoplasmic compartment. Only one equation, accounting for uniform production and degradation, remains to be solved. At the onset of the following interphase, the number of compartments increases and compartment volumes sizes are updated.